Quantum energy teleportation in a quantum Hall system

Go Yusa,* Wataru Izumida, and Masahiro Hotta
Department of Physics, Tohoku University, Sendai 980-8578, Japan
(Received 13 January 2011; revised manuscript received 5 July 2011; published 26 September 2011)

We propose an experimental method for a quantum protocol termed quantum energy teleportation (QET), which allows energy transportation to a remote location without physical carriers. Using a quantum Hall system as a realistic model, we discuss the physical significance of QET and estimate the order of energy gain using reasonable experimental parameters.

DOI: 10.1103/PhysRevA.84.032336 PACS number(s): 03.67.−a, 73.43.−f

I. INTRODUCTION

The phenomenon of quantum teleportation (QT) has been experimentally demonstrated in quantum optics [1,2]. But, as is well known, this protocol can teleport only *information* (i.e., quantum-mechanical information or quantum states) and not *physical objects*. Thus, this protocol cannot teleport energy because that requires a physical entity to act as an energy carrier. For example, electricity is transported over power transmission lines by electromagnetic waves that act as the carrier. Recently, however, one of the authors proposed a quantum protocol termed quantum *energy* teleportation (QET) that avoids the problem by using classical information instead of energy carriers [3]. In this counterintuitive protocol, the counterpart of the classical transmission line is a quantum-mechanical many-body system in the vacuum state (i.e., a correlated system formed by vacuum state entanglement [4]). The key lies in using this correlated system (hereinafter, the quantum correlation channel) to exploit the zero-point energy of the vacuum state, which stems from zero-point fluctuations (i.e., nonvanishing vacuum fluctuations) originating from the uncertainty principle. This energy, however, cannot be extracted conventionally [5] as that would require a state with lower energy than vacuum—a contradiction. In fact, no local operation can extract energy from vacuum but instead, must inject energy; this property is called passivity [6]. According to QET, however, if we only limit the *local* vacuum state instead of all the vacuum states, the passivity of the local vacuum state can be destroyed, and a part of the zero-point energy, in fact, can be extracted.

As schematically illustrated in Fig. 1, a QET system to transfer energy from subsystem A to B consists of four elements: (i) a quantum correlation channel, (ii) a local measurement system for subsystem A defined on the quantum correlation channel, (iii) a classical channel for communicating the measurement result, and (iv) a local operation system for subsystem B. Essentially, QET can be regarded as a quantum feedback protocol implemented via local operations and classical communication (LOCC). The procedure is as follows: First, we measure the local-field fluctuations at subsystem A. The obtained result includes information about local fluctuations at subsystem B because of the vacuum state entanglement via the quantum correlation channel [4]. This is because the kinetic-energy term in the field Hamiltonian generates the entanglement and provides partial correlation between local vacuum fluctuations. Thus, owing to passivity of the vacuum state, the measurement causes some energy (E_A) to be injected into subsystem A. Next, the obtained result is communicated to subsystem B via a classical channel. Since the measurement performed at subsystem A is *local*, subsystem B remains in a local vacuum state. As mentioned above, if a good local operation is performed at subsystem B using the information gained at subsystem A, it will be possible to extract some amount of the zero-point energy of subsystem B, E_B. Thus, this protocol only gives permission to use the otherwise unavailable energy at B. If we define teleportation as a process of transferring energy to a remote location without a physical energy carrier, we can say that energy is teleported by this protocol.

Although the validity of this protocol has been confirmed *mathematically*, its *physical* significance remains questionable: What type of physical system is necessary for implementing QET? What is the composition of the quantum correlation channel? Can significant amounts of energy be teleported? Unfortunately, all past proposals for experimental verification of QET cannot teleport sufficient amounts of energy to be measured with the present technology [7,8]. Here, we discuss a more realistic possible implementation and estimate the order of the teleported energy using reasonable experimental parameters.

II. OVERVIEW OF QET PROTOCOL IN THE QUANTUM HALL SYSTEM

Verification of QET in a realistic system requires the following: (i) a dissipationless system, (ii) a quantum correlation channel with a macroscopic correlation length, (iii) detection and operation schemes for well-defined fluctuations in the vacuum state, and (iv) a suitable implementation of LOCC.

To this end, we consider a quantum Hall (QH) system as a potential candidate. The QH effect is observed in two-dimensional (2D) electron systems in semiconductors subjected to a strong perpendicular magnetic field [9]. The QH system satisfies requirement (i) because the QH effect does not offer any resistance. Furthermore, in this system, quasi-one-dimensional channels, called edge channels, appear at the boundary of the 2D incompressible region of the QH system (i.e., QH bulk). Such an edge channel can behave as a *chiral* Luttinger liquid [10], along which electric current flows in a unidirectional manner. This attribute is

*yusa@m.tohoku.ac.jp

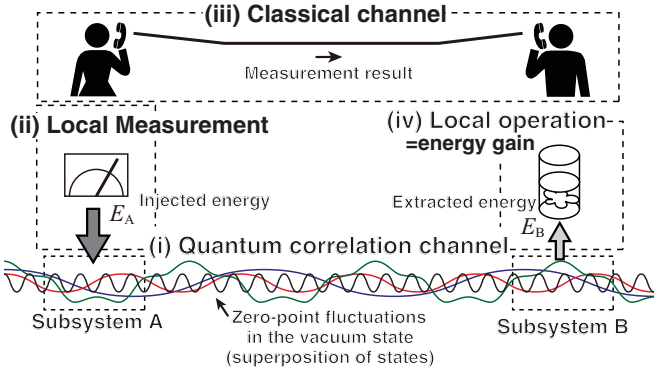

FIG. 1. (Color online) Schematic of the QET protocol.

indicative of the chirality of the edge channel. Moreover, in experiments, the edge channel shows power-law behaviors and does not have a specific decay length [11,12], preferable for fairly long-distance teleportation. Thus, an edge channel satisfies requirement (ii). Furthermore, an edge channel can be characterized universally by charge fluctuations described by a gapless free-boson field in the vacuum state, independent of the detailed structures of the QH bulk state. Therefore, the target zero-point fluctuation is the fluctuation of the charge density wave (i.e., a magnetoplasmon [13]) propagating in a unidirectional manner along an edge channel). This implies that, owing to the Coulomb interaction, a conventional capacitor can be used as a sensitive probe and control method for detecting and manipulating zero-point fluctuations of vacuum. Given these facts, it can be said that (iii) is satisfied. Last, for a QH system, semiconductor nanotechnology can be used to design on-chip LOCC, thus, satisfying requirement (iv).

As shown in Fig. 2, element (i), i.e., the quantum correlation channel, is the left-going edge channel S. To produce the vacuum state, S should be connected to an ideal electric ground, and experiments should be performed at low temperatures—on the order of millikelvin (mK). Regions A and B, physically corresponding to subsystems A and B, respectively, are defined by fabricating micrometer-scale metal gate electrodes (i.e., a microscopic capacitor) on S.

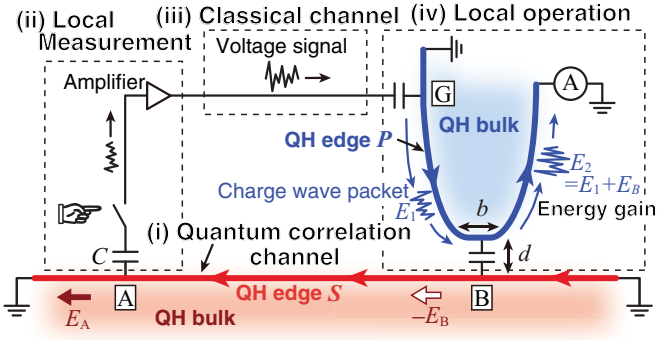

FIG. 2. (Color online) Schematic of the QH system used in this paper. Edge channels S and U are formed at the boundaries of QH bulk regions S and U, respectively. The arrows indicate the directions of the propagation of charge waves.

Element (ii), used for local measurement of the zero-point fluctuations (i.e., charge fluctuations), comprises a metal gate electrode fabricated on S at region A as well as an amplifier and a switch. The input resistance R of the amplifier and capacitance C between S and the gate electrode at region A constitute an RC circuit. When the switch is turned on, the information on the charge fluctuations in S is imprinted on the quantum voltage fluctuations of the electric circuit via the Coulomb interaction and then is enhanced by the amplifier. Here, the on-chip electrical circuit serves the function of the voltmeter shown in the schematic in Fig. 1. As explained later, we can assume that this RC circuit and amplifier can operate fast enough, and the circuit can be considered as performing a positive-operator-valued-measure-(POVM)-type measurement [11]. The amplified signal υ (i.e., measurement result) is transferred through a classical channel [element (iii)], which corresponds to an electric wire.

Element (iv), used for the local operation, includes another edge channel P placed such that P and S approach each other at region B. It also consists of a metal gate electrode fabricated on P at region G and a measurement instrument, such as a picoammeter (Fig. 2).

The experimental procedure is as follows: First, we cool down the entire system, except the measurement instruments, to the lowest temperature possible (on the order of several mK) to achieve the vacuum state. Next, we only turn on the switch for a period of τ_m. When a voltage signal υ arrives at region G, it excites a charge wave packet on P via capacitive coupling. Because of the chirality of the edge channel, the charge wave packet travels in a unidirectional manner along P, carrying energy E_1 toward region B, where the wave packet interacts with the zero-point fluctuation of S [14]. Then, the energy carried by the wave packet changes from E_1 to E_2. Finally, we measure the signal with the picoammeter connected to P and, thereby, estimate the energy carried by the wave packet. This is a unit cycle of a single-shot measurement. We may repeat this single-shot measurement a sufficient number of times to generate meaningful statistics. Finally, we can use the results to estimate the average energy $\langle E_2 \rangle$ carried by the wave packets. To verify that QET is actually occurring, we must also perform a control experiment in which region G is disconnected from the classical channel and instead, is connected to a signal generator to excite wave packets *independent* of υ. If wave packets are created by the signal generator (i.e., no information about υ is communicated), they will inject energy into S because of the passivity of the vacuum state [6]. Thus, $E_B = E_2 - E_1$ will be negative. However, in our system, since wave packets explicitly depend on υ, passivity is disturbed, and $\langle E_2 \rangle$ can take a positive value; in other words, positive energy is extracted from the zero-point fluctuations of S. Finally, if $\langle E_2 \rangle$ is larger in the QET experiment than in the control, we can conclude that the QET theory is valid—energy is teleported from A to B without physical carriers to transport that energy. In what follows, we prove this argument theoretically and estimate E_B by setting the experimental parameters $R \sim 10\ \mathrm{k}\Omega$ [15]; $C \sim 10$ fF; and $v_g \sim 10^6$ m/s [16,17], where v_g is the group velocity of a charge density wave. Length b of regions G and B and the length of region A are approximated by a typical length scale of $l \sim 10\ \mu$m.

III. QET FORMULATION IN THE QH SYSTEM

A. Formulation of chiral edge channel and local measurement of charge fluctuations

Here, we discuss the chiral field of the edge channels. Details on the treatment of the chiral field can be found in the literature [9]. Let us start the detailed discussion with a model of the edge channel S. The chiral field operator $\varrho_S(x)$ satisfies a commutation relation $[\varrho_S(x),\varrho_S(x')] = i\frac{\nu}{2\pi}\partial_x\delta(x-x')$. The energy density operator of $\varrho_S(x)$ is written as

$$\varepsilon_S(x) = \frac{\pi\hbar v_g}{\nu_S}:\varrho_S(x)^2:,$$

where ν_S is the Landau level filling factor of S and : : denotes normal ordering, which makes the expectation value of $\varepsilon_S(x)$ zero for the vacuum state $|0_S\rangle$; $\langle 0_S|\varepsilon_S(x)|0_S\rangle = 0$. The free Hamiltonian of S is given by $H_S = \int_{-\infty}^{\infty}\varepsilon_S(x)dx$. The eigenvalue of the vacuum state vanishes: $H_S|0_S\rangle = 0$. If the vacuum state is not entangled, the two-point correlation function of $\langle 0_S|\varrho_S(x_A)\varrho_S(x_B)|0_S\rangle$ with $x_A \neq x_B$ is exactly zero. However, this entangled vacuum state provides a nontrivial correlation,

$$\langle 0_S|\varrho_S(x_A)\varrho_S(x_B)|0_S\rangle = -\frac{\nu_S}{4\pi^2(x_A-x_B)^2}.$$

This correlation function can be calculated by using creation and annihilation operators of the free field. Taking region A for $x \in [a_-,a_+]$, we adopt the RC-circuit-detector model proposed by Fève *et al.* [18] to measure the voltage induced by the zero-point fluctuations of $\varrho_S(x)$. The charge fluctuation at A is estimated as

$$Q_S(t) = e\int_{-\infty}^{\infty}\varrho_S(x+v_g t)w_A(x)dx, \tag{1}$$

with a window function $w_A(x)$ that equals 1 in $x \in [a_-,a_+]$ and decays rapidly outside A. In this model [18], the voltage at the contact point between the detector and S is given by $V(t) = \frac{1}{C}[Q_S(t) - Q(t)]$, where $Q(t)$ is the charge of the capacitor. The coupled Hamiltonian of S and the RC circuit can be diagonalized directly, enabling analytical estimation of various physical quantities [18]. For example, the quantum noise of the voltage $V(t)$ is described by an operator $\hat{V}$ defined by

$$\hat{V} = -\sqrt{\frac{\hbar}{\pi RC^2}} \times \int_0^{\infty} d\omega\left[\frac{\sqrt{\omega}}{\omega - \frac{1}{iRC}}a_{\rm in}(\omega) + \frac{\sqrt{\omega}}{\omega + \frac{1}{iRC}}a_{\rm in}^{\dagger}(\omega)\right], \tag{2}$$

where $a_{\rm in}(\omega)[a_{\rm in}(\omega)^{\dagger}]$ is the annihilation (creation) operator of excitation of the charge density wave in the local-measurement RC circuit and $[a_{\rm in}(\omega),a_{\rm in}(\omega')^{\dagger}] = \delta(\omega-\omega')$. Prior to the measurement (i.e., the signal input from S to the detector), $V(t=-0)$ equals $\hat{V}$. Using the fast detector condition ($RC \ll l/v_g$), the voltage after the measurement is computed as

$$V(t=+0) = \hat{V} + R\dot{Q}_S(0), \tag{3}$$

where $R\dot{Q}_S(0)$ denotes the voltage shift induced by the signal and the dot in $\dot{Q}_S(0)$ stands for the time derivative. Using Eq. (2), the amplitude ΔV of $\hat{V}$ in the vacuum state $|0_{RC}\rangle$ of the RC circuit can be estimated as

$$\Delta V = \sqrt{\langle 0_{RC}|\hat{V}^2|0_{RC}\rangle} \sim \sqrt{\frac{\hbar}{RC^2}},$$

which is expected to be on the order of 10 μV. From Eq. (1), the root-mean-square value of the voltage shift $\sqrt{\langle 0_S|[R\dot{Q}_S(0)]^2|0_S\rangle}$ is estimated to be on the order of 100 μV, showing that the quantum fluctuations of the edge current are detectable.

Now, we estimate the corresponding measurement operators [19] of this voltage measurement. Clearly, this is difficult to achieve with sufficient accuracy with a microscopic model. However, after the amplification of the quantum noise of the voltage $V(t)$, the signal becomes macroscopic and classical. Thus, we may estimate the measurement operators of the macroscopic system comprising subsystem A, the amplifier, and the electric wire by reducing the measurement to the pointer basis proposed by von Neumann [20]. For this, let us begin with a gedankenexperiment in which a high-speed voltage meter is connected to the amplifier. Thus, the position of the meter pointer instantaneously shifts according to the signal strength. Assume that the pointer shift is equal to Eq. (3). In the same manner as that used by von Neumann [20], we can treat the macroscopic system including this voltage meter with quantum mechanics, even though the meter is macroscopic and classical. Therefore, the readout of the meter pointer can be treated as a kind of quantum measurement, which can be described by measurement operators M_v [19] with the output value of v. The shift of the meter pointer $R\dot{Q}_S(0)$ in Eq. (3) can be reproduced by a macroscopic measurement Hamiltonian given by

$$H_m(t) = \hbar\delta(t)R\dot{Q}_S(0)P_{\hat{V}},$$

where $P_{\hat{V}}$ is the conjugate momentum operator of $\hat{V}$. In fact, the time evolution generated by this effective Hamiltonian is given by

$$U_m = {\rm T}\exp\left(-\frac{i}{\hbar}\int_{-0}^{+0}H_m(t)dt\right) = \exp[-iR\dot{Q}_S(0)P_{\hat{V}}],$$

with time-ordered exponentiation, T exp, of the time-dependent Hamiltonian and reproduces Eq. (3) as follows:

$$U_m^{\dagger}\hat{V}U_m = V(t=+0) = \hat{V} + R\dot{Q}_S(0).$$

We are able to derive the measurement operators M_v by using U_m. First, by using the eigenvalue v of $\hat{V}$ ($\hat{V}|v\rangle = v|v\rangle$), we can assume the initial wave function of the quantum pointer in the v representation as

$$\Psi_i(v) \propto \exp\left[-\frac{1}{4\,\Delta V^2}v^2\right],$$

whereas, the wave function after the measurement is translated as

$$\Psi_f(v) \propto \exp\left[-\frac{1}{4\,\Delta V^2}[v - R\dot{Q}_S(0)]^2\right],$$

using U_m. Next, after turning the measurement interaction on (i.e., turning the switch on), we perform a projective measurement of $\hat{V}$ to obtain an eigenvalue v of $\hat{V}$. This

reduction analysis proves the measurement operator M_υ to be $\Psi_f(\upsilon)$,

$$M_\upsilon = \left(\frac{1}{2\pi\,\Delta V^2}\right)^{1/4} \exp\left[-\frac{1}{4\,\Delta V^2}[\upsilon - R\dot{Q}_S(0)]^2\right].$$

The corresponding POVM is given by $\Pi_\upsilon = M_\upsilon^\dagger M_\upsilon$ and satisfies the standard sum rule: $\int_{-\infty}^{\infty}\Pi_\upsilon d\upsilon = I_S$, where I_S is the identity operator of the Hilbert space of $\varrho_S(x)$. The emergence probability density of the result being υ is $p(\upsilon) = \langle 0_S|\Pi_\upsilon|0_S\rangle$. The postmeasurement state of $\varrho_S(x)$ corresponding to the result υ is computed as $M_\upsilon|0_S\rangle$ up to the normalization constant. Hence, the average state of $\varrho_S(x)$, right after the measurement, is given by

$$\rho_1 = \int_{-\infty}^{\infty} M_\upsilon|0_S\rangle\langle 0_S|M_\upsilon^\dagger d\upsilon.$$

The amount of energy injected by the measurement is calculated as

$$\begin{aligned} E_A &= \int_{-\infty}^{\infty}\langle 0_S|M_\upsilon^\dagger H_S M_\upsilon|0_S\rangle d\upsilon \\ &= \frac{\hbar v_g \nu_S}{4\pi}\left(\frac{e v_g R}{2\,\Delta V}\right)^2 \int_{-\infty}^{\infty} dx\left[\partial_x^2 w_A(x)\right]^2. \end{aligned}$$

Using the experimental parameters mentioned earlier, E_A can be estimated to be on the order of 1 meV for $\nu_S \sim 3$. Since the meter that we consider is sufficiently macroscopic such that quantum effects can be neglected, the estimation of M_υ and E_A remains unchanged even if we directly send the amplified classical signal to region G without the voltage meter we assumed above.

B. Formulation of local operation and estimated energy gain at B

Now, let us turn to the edge channel P and discuss how wave packets can be excited at G (i.e., how to send the measurement result to B). After the measurement result, υ is amplified and is transferred to region G as a voltage signal through the wire; the voltage signal (i.e., the electric field) excites a charge wave packet of $\varrho_P(y)$. Here, $\varrho_P(y)$ is the chiral field operator, the counterpart of $\varrho_S(x)$ in the edge channel S. In other words, by performing a υ-dependent unitary operation U_υ on the vacuum state $|0_P\rangle$ of $\varrho_P(y)$, a localized right-going coherent state is generated: $|\upsilon_P\rangle = U_\upsilon|0_P\rangle$ in a region with $y \in [b_- - L, b_+ - L]$, where L is the distance between regions G and B. The length $b_+ - b_-$ of region B is given by b ($\sim l$). This operation is realized by applying an electric field with a strength proportional to the measurement υ on the edge channel P. Such a unitary operation is experimentally feasible, since charge coherent states have been demonstrated experimentally in semiconductor quantum dots [21]. However, in order to realize QET experimentally, proper tuning of the unitary operation U_υ is important. Here, let $F_\upsilon(y,t)$ be the electric potential (i.e., classical external potential) produced by the amplified voltage signal at region G. By using $F_\upsilon(y,t)$, the interaction Hamiltonian of U_υ is given by a linear term of $\varrho_P(y)$ as

$$H_\upsilon = \int_{b_- - L}^{b_+ - L} F_\upsilon(y,t)\varrho_P(y)dy. \tag{4}$$

Taking negative values of $F_\upsilon(y,t)$ ensures that the sign of E_B is positive. A standard inverting amplifier allows us to achieve this sign reversal for $F_\upsilon(y,t)$ with respect to υ. Now, we assume the potential $F_\upsilon(y,t)$ is as follows, and then, we discuss how to generate this potential experimentally:

$$F_\upsilon(y,t) = -\frac{\pi\hbar}{\nu_P\Delta V}\upsilon\lambda_B(y)\delta_{\tau_m}(t - t_o),$$

where $\delta_{\tau_m}(t - t_o)$ is a real localized function at t_o with a short-time width τ_m satisfying $\lim_{\tau_m\to 0}\delta_{\tau_m}(t - t_o) = \delta(t - t_o)$. In addition, $\lambda_B(y)$ is a window function related to the total number of excited electrons and quasiholes from the vacuum state. In other words, the excited wave packet, which extends over the region with $[b_- - L, b_+ - L]$, contains the same order of $\lambda_B(y)$. Therefore, $\lambda_B(y)$ is related to the shape of the metal gate electrode at region G. By using $[\varrho_P(y),\varrho_P(y')] = -i\frac{\nu_P}{2\pi}\partial_y\delta(y - y')$, the wave form is computed as $\langle\upsilon_P|\varrho_P(y)|\upsilon_P\rangle = \frac{\upsilon}{2\,\Delta V}\partial_y\lambda_B(y)$. Because the charge density $\langle\upsilon_P|\varrho_P(y)|\upsilon_P\rangle$ can be measured directly in experiments, $\lambda_B(y)$ also is measured depending on the design of the gate electrode at G. Here, we take the amplitude of $\lambda_B(y)$ to be on the order of 10. To clarify the relation between $F_\upsilon(y,t)$ and the voltage signal υ, let us analyze the gain α of the amplifier. By setting α as

$$\alpha = \frac{\pi\hbar}{\nu_P\Delta V\,\tau_m}\max_y\lambda_B(y),$$

the potential $F_\upsilon(y,t)$ is order estimated as

$$O(F_\upsilon) = \alpha O(\upsilon) = \alpha\,\Delta V.$$

This suggests that the order of the potential is simply proportional to the quantum noise ΔV multiplied by the gain. If τ_m is of nanosecond order, $F_\upsilon(y,t)$ is on the order of 10 μV. Thus, the amplitude and the spatial profile of $F_\upsilon(y,t)$ experimentally are tunable by the gain of the amplifier and the shape of the gate electrode, respectively. Using the approximation $\tau_m \sim 0$, this simple interaction in Eq. (4) generates a displacement operator given by

$$U_\upsilon = \exp\left(\frac{\pi i\upsilon}{\nu_P\Delta V}\int_{b_- - L}^{b_+ - L}\lambda_B(y)\varrho_P(y)dy\right).$$

The composite state of S and P at a time T, when generation of a charge wave packet completes, is calculated as

$$\rho_{\rm SP} = \int_{-\infty}^{\infty} d\upsilon\, e^{-(iT/\hbar)H_S}M_\upsilon|0_S\rangle\langle 0_S|M_\upsilon^\dagger e^{(iT/\hbar)H_S}\otimes|\upsilon_P\rangle\langle\upsilon_P|.$$

This state is the scattering input state for the Coulomb interaction between S and P. Then, the charge wave packet evolves into region B by the free Hamiltonian,

$$H_B = \frac{\pi\hbar\upsilon}{\nu_P}\int_{-\infty}^{\infty}:\varrho_P(y)^2:dy.$$

The average value of the energy of the wave packet is $E_1 = Tr[H_B\rho_{\rm SP}]$. This is calculated as

$$E_1 = \frac{\pi\hbar v_g}{\nu_P}\int_{-\infty}^{\infty}[\partial_y\lambda_B(y)]^2dy\left[\langle 0_S|G_S^2|0_S\rangle + \frac{1}{4}\right],$$

where

$$G_S = -\frac{e v_g R}{2\,\Delta V}\int_{-\infty}^{\infty}\varrho_S(x)\partial_x w_A(x)dx.$$

Here, E_1 is estimated to be on the order of 10 meV for v_S and v_P of 3 and 6, respectively. At region B, the two channels S and P interact with each other via Coulomb interaction such that

$$H_{\rm int} = \frac{e^2}{4\pi\epsilon}\int_{b_-}^{b_+} dx \int_{b_-}^{b_+} dy\, \varrho_S(x) f(x,y) \varrho_P(y).$$

Here, ϵ is $10\epsilon_0$ for the host semiconductor (e.g., gallium arsenide, GaAs), where ϵ_0 is the dielectric constant of vacuum. The function $f(x,y)$ is given by $\frac{1}{\sqrt{(x-y)^2+d^2}}$, and d ($\sim l$) is the separation length between the two edge channels at B. After exchanging energy with $\varrho_S(x)$, the energy carried by the wave packet becomes E_2. The energy gain $E_B = E_2 - E_1$ is estimated by the lowest-order perturbation theory in terms of $H_{\rm int}$ as follows:

$$\begin{aligned} E_B = -i\frac{e^2 v_g}{4\epsilon v_S}\int_{-\infty}^{\infty} dz \int_{b_-}^{b_+} dx_B \int_{b_-}^{b_+} dy_B f(x_B, y_B) \\ \times \int_{-\infty}^{\infty} dt \int_{-\infty}^{\infty} d\upsilon \langle 0_S| M_\upsilon'^{\dagger} \varrho_S(x_B + v_g t) M'_\upsilon |0_S\rangle \\ \times \langle \upsilon'_P| [\varrho_B(z - v_g t_f)^2, \varrho_B(y_B - v_g t)] |\upsilon'_P\rangle, \end{aligned}$$

where $M'_\upsilon = U_S(t_i - T)^\dagger M_\upsilon U_S(t_i - T)$ and $|\upsilon'_P\rangle = U_B(t_i)^\dagger |\upsilon_B\rangle$. By substituting the commutation relation given by $[\varrho_B(z)^2, \varrho_B(y_B)] = -i\frac{v_S}{\pi}\partial\delta(z - y_B)\varrho_B(z)$ and performing the z integral, we obtain the following relation:

$$\begin{aligned} E_B = \frac{e^2 v_g}{4\pi\epsilon}\int_{b_-}^{b_+} dx_B \int_{b_-}^{b_+} dy_B f(x_B, y_B) \\ \times \int_{-\infty}^{\infty} dt\, \partial^2 \lambda_B[y_B - v_g(t - t_i)] \\ \times \int_{-\infty}^{\infty} \upsilon \langle 0_S| M_\upsilon'^{\dagger} \varrho_S(x_B + v_g t) M'_\upsilon |0_S\rangle d\upsilon. \end{aligned}$$

Note that the last integral is computed as

$$\begin{aligned} \int_{-\infty}^{\infty} \upsilon \langle 0_S| M_\upsilon'^{\dagger} \varrho_S(x_B + v_g t) M'_\upsilon |0_S\rangle d\upsilon \\ = -\frac{e\upsilon R}{4\,\Delta V}\int_{-\infty}^{\infty} d\bar{x}_A \partial w_A(\bar{x}_A) \\ \times \Delta[\bar{x}_A - x_B - v_g(t + T - t_i)] + \text{c.c.}, \end{aligned}$$

where

$$\Delta(x) = \frac{v_S}{4\pi^2}\int_0^{\infty} dk\, k \exp(-ikx).$$

For the t integral of E_B, let us use the Fourier transform $\partial^2\lambda_B$ in E_B as

$$\partial^2\lambda_B(y) = -\frac{1}{2\pi}\int_{-\infty}^{\infty} k'^2 \tilde{\lambda}_B(k') e^{ik'y} dk'.$$

Using $\int_{-\infty}^{\infty} dt\, \exp[-i(k' \pm k)v_g t] = \frac{2\pi}{v_g}\delta(k' \pm k)$, E_B is estimated as

$$\begin{aligned} E_B = \frac{3e^3 \upsilon R v_S}{4\pi^3\epsilon\,\Delta V}\int_{a_-}^{a_+} d\bar{x}_A \int_{b_-}^{b_+} d\bar{y}_B \int_{b_-}^{b_+} dx_B \int_{b_-}^{b_+} dy_B \\ \times \frac{1}{\sqrt{(x_B - y_B)^2 + d^2}} \\ \times \frac{w_A(\bar{x}_A)\lambda_B(\bar{y}_B - L)}{(x_B + y_B - \bar{x}_A - \bar{y}_B + L + v_g T)^5}, \end{aligned} \tag{5}$$

where $v_g T = O(10^{-2}L)$. The parameter $L + v_g T [= O(L)]$ corresponds to the distance between A and B. Thus, the energy output E_B is estimated as

$$E_B \sim \frac{e^2\lambda_B}{4\pi\epsilon l}\frac{e v_g R}{l\,\Delta V}\left(\frac{l}{L}\right)^5. \tag{6}$$

Here, it should be emphasized that a positive function $\lambda_B(\bar{y}_B + L)$ guarantees positive E_B. Obviously, from Eq. (6), an increase in L rapidly degrades the magnitude of E_B (e.g., $E_B \sim 1\ \mu$eV for $L \sim 4l$). Nevertheless, for $L \sim 2l$, E_B attains a value on the order of 100 μeV. This is much larger than the thermal energy $\sim 1\ \mu$eV at a temperature of ~ 10 mK, at which experiments on the QH effect are often performed (using a dilution refrigerator). Note here that, to estimate the actual value of E_B, we need to know E_1 since the energy, which can be measured by the setup in Fig. 2, is E_2 ($= E_B + E_1$). E_1 can be estimated by letting d be sufficiently large [22].

To observe E_B experimentally, we turn on the switch and measure the current passing through the edge channel P once (single-shot measurement). The relation

$$\varepsilon = \frac{\pi\hbar}{v_P e^2 v_g} j^2,$$

between the energy density ε and the current j gives an energy density of 10 μeV/μm, which corresponds to a current of 10 nA. This current can be detected experimentally using a picoammeter. To verify that energy is extracted at B, a sufficient number of single-shot current measurements should be conducted (by switching the circuit on and off) to generate meaningful statistics for the POVM measurement. In this process, the electrical noise, which can be introduced in the classical channel, is averaged out and, thus, does not affect $\langle E_B\rangle$. Note here that $(l/L)^5$ dependence of the estimated E_B is based on the first-order perturbation theory, and the dependence might be slower than in higher-order approximations or in a framework of more suitable local operations. Careful discussions are needed for optimizing the experimental setup to obtain maximum E_B.

IV. DISCUSSION AND CONCLUSION

We now examine energy conservation and dynamics in the system. As we have shown, the extraction of E_B from the local vacuum state requires measurement (energy injection) at A. What is the source of E_A? We consider a POVM measurement so that switching on the RC circuit causes energy E_A to be injected into S. Therefore, if the switch is electrically operated, a battery may provide E_A to drive the switching device [23]. After extracting E_B, the total energy $E_A - E_B$ of the system

will be non-negative, as expected, because $E_A > E_B$. According to the local energy conservation laws, the transfer of energy E_B from S to P results in a negative average quantum energy density around B. This negative energy density is obtained by squeezing the amplitude of the zero-point fluctuation to less than that of the vacuum state during the interaction [24]. Then, $-E_B$ and E_A will flow unidirectionally along the edge toward the downstream electrical ground with identical velocities of v_g, and S around region B will remain in a local vacuum state with zero energy density.

Although no studies have been conducted on QET in QH systems, several successful experimental studies have been conducted in quantum optics by introducing LOCC including QT [1,2]. Light is a massless electromagnetic field; however, at present, it is difficult to directly measure the zero-point fluctuations of light owing to the lack of an appropriate interaction, such as the Coulomb interaction in QH systems. Thus, our QH system is considered to be very suitable for demonstrating the QET protocol.

QET can be interpreted in terms of information thermodynamics as a quantum version of Maxwell's demon [25]; in particular, two demons cooperatively extract energy from quantum fluctuations at zero temperature. Moreover, this type of quantum feedback is relevant to black-hole entropy, whose origin has been discussed often in string theory [26], because energy extraction from a black hole reduces the horizon area (i.e., the entropy of the black hole [27]).

In conclusion, theoretically, we have shown the implementation of QET and estimated the order of the energy gain E_B in a QH system using reasonable experimental parameters.

ACKNOWLEDGMENTS

The authors thank K. Akiba and T. Yuge for fruitful discussions. G.Y., W.I., and M.H. are supported by Grants-in-Aid for Scientific Research (Grant Nos. 21241024, 22740191, and 21244007, respectively) from the Ministry of Education, Culture, Sports, Science and Technology (MEXT), Japan. W.I. and M.H. are partly supported by the Global COE Program of MEXT, Japan. G.Y. is partly supported by the Sumitomo Foundation.

[1] C. H. Bennett, G. Brassard, C. Crépeau, R. Jozsa, A. Peres, and W. K. Wootters, Phys. Rev. Lett. **70**, 1895 (1993).
[2] D. Bouwmeester *et al.*, Nature (London) **390**, 575 (1997); A. Furusawa *et al.*, Science **282**, 706 (1998).
[3] M. Hotta, Phys. Lett. A **372**, 5671 (2008); J. Phys. Soc. Jpn. **78**, 034001 (2009); Y. Nambu and M. Hotta, Phys. Rev. A **82**, 042329 (2010).
[4] B. Reznik, Found. Phys. **33**, 167 (2003); J. Silman and B. Reznik, Phys. Rev. A **71**, 054301 (2005).
[5] In fact, this energy is responsible for the Casimir force between two parallel conducting plates; however, it is impossible to locally extract this force from the vacuum state without changing the boundary conditions of the field, such as in the Casimir effect.
[6] W. Pusz and S. L. Woronowicz, Commun. Math. Phys. **58**, 273 (1978).
[7] M. Hotta, Phys. Rev. A **80**, 042323 (2009).
[8] M. Hotta, J. Phys. A: Math. Theor. **43**, 105305 (2010).
[9] D. Yoshioka, *The Quantum Hall Effect* (Springer, Berlin, 2002).
[10] X. G. Wen, Phys. Rev. B **43**, 11025 (1991).
[11] A. M. Chang, L. N. Pfeiffer, and K. W. West, Phys. Rev. Lett. **77**, 2538 (1996).
[12] M. Grayson, D. C. Tsui, L. N. Pfeiffer, K. W. West, and A. M. Chang, Phys. Rev. Lett. **80**, 1062 (1998).
[13] S. J. Allen Jr., H. L. Störmer, and J. C. M. Hwang, Phys. Rev. B **28**, 4875 (1983).
[14] It should be stressed that, since the edge current of S flows only to the left and that the upstream of subsystem B is connected to an ideal electric ground, the zero-point fluctuations at subsystem B are not affected by events that occur in the downstream regions. Thus, subsystem B always remains in the local vacuum state before the local operation at B.
[15] The characteristic impedance of wires is matched to R.
[16] R. C. Ashoori, H. L. Störmer, L. N. Pfeiffer, K. W. Baldwin, and K. West, Phys. Rev. B **45**, 3894 (1992).
[17] H. Kamata, T. Ota, K. Muraki, and T. Fujisawa, Phys. Rev. B **81**, 085329 (2010).
[18] G. Fève, P. Degiovanni, and T. Jolicoeur, Phys. Rev. B **77**, 035308 (2008).
[19] M. A. Nielsen and I. L. Chuang, *Quantum Computation and Quantum Information* (Cambridge University Press, Cambridge, UK, 2000).
[20] J. von Neumann, *Mathematical Foundations of Quantum Mechanics* (Princeton University Press, Princeton, 1955).
[21] T. Hayashi, T. Fujisawa, H. D. Cheong, Y. H. Jeong, and Y. Hirayama, Phys. Rev. Lett. **91**, 226804 (2003).
[22] For example, we place a metal gate electrode between the two edge channels. By applying a negative voltage to the gate, the 2D electron density can be depleted locally. In this fashion, the effective distance d between the two edge channels can be controlled continuously. Such a technique is commonly used in experiments related to semiconductor nanostructures.
[23] Unlike the local measurement, which can be connected to S by the switch only during the measurement, the local operation is always attached to S. In the presented analysis, we can omit the modification effects induced by the existence of U adjacent to S because such a backaction effect appears only in higher correction terms of the perturbation.
[24] Such emergence of negative energy density is widely discussed in quantum-field theory. For example, one of the most simple cases involves the linear superposition of the vacuum state and the multiparticle states of a quantum field [28].
[25] W. H. Zurek, in *Frontiers of Nonequilibrium Statistical Physics*, edited by G. T. Moore and M. O. Scully (Plenum, New York, 1984), p. 151; S. Lloyd, Phys. Rev. A **56**, 3374 (1997); T. Sagawa and M. Ueda, Phys. Rev. Lett. **100**, 080403 (2008).
[26] A. Strominger and C. Vafa, Phys. Lett. B **379**, 99 (1996); A. Sen, Gen. Relativ. Gravit. **40**, 2249 (2008).
[27] M. Hotta, Phys. Rev. D **81**, 044025 (2010).
[28] L. H. Ford, Proc. R. Soc. London, Ser. A **364**, 227 (1978).